1521-0111/83/5/1099–1108$25.00
MOLECULAR PHARMACOLOGY

http://dx.doi.org/10.1124/mol.112.084368
Mol Pharmacol 83:1099–1108, May 2013

A Newly Synthesized Sinapic Acid Derivative Inhibits Endothelial Activation In Vitro and In Vivo[S]

Xiaoyun Zeng, Jinhong Zheng, Chenglai Fu, Hang Su, Xiaoli Sun, Xuesi Zhang, Yingjian Hou, and Yi Zhu

Cardiovascular Research Center (X.Ze., H.S., X.Zh., Y.Z.) and Department of Chemistry (J.Z.), Shantou University Medical College, Shantou, Guangdong, China; Department of Physiology and Pathophysiology, Peking University Health Sciences Center, Beijing, China (C.F., X.S., Y.H.); and Department of Physiology and Pathophysiology, Tianjin Medical University, Tianjin, China (Y.Z.)

Received December 11, 2012; accepted March 7, 2013

ABSTRACT

Inhibition of oxidative stress and inflammation in vascular endothelial cells (ECs) may represent a new therapeutic strategy against endothelial activation. Sinapic acid (SA), a phenylpropanoid compound, is found in natural herbs and high-bran cereals and has moderate antioxidant activity. We aimed to develop new SA agents with the properties of antioxidation and blocking EC activation for possible therapy of cardiovascular disease. We designed and synthesized 10 SA derivatives according to their chemical structures. Preliminary screening of the compounds involved scavenging hydroxyl radicals and 2,2-diphenyl-1-picrylhydrazyl (DPPH$^{\cdot}$), croton oil-induced ear edema in mice, and analysis of the mRNA expression of adhesion molecules in ECs. 1-Acetyl-sinapic acyl-4-(3′-chlorine-)benzylpiperazine (SA9) had the strongest antioxidant and anti-inflammatory activities both in vitro and in vivo. Thus, the effect of SA9 was further studied. SA9 inhibited tumor necrosis factor α-induced upregulation of adhesion molecules in ECs at both mRNA and protein levels, as well as the consequent monocyte adhesion to ECs. In vivo, result of face-to-face immunostaining showed that SA9 reduced lipopolysaccharide-induced expression of intercellular adhesion molecule-1 in mouse aortic intima. To study the molecular mechanism, results from luciferase assay, nuclear translocation of NF-κB, and Western blot indicated that the mechanism of the anti-inflammatory effects of SA9 might be suppression of intracellular generation of ROS and inhibition of NF-κB activation in ECs. SA9 is a prototype of a novel class of antioxidant with anti-inflammatory effects in ECs. It may represent a new therapeutic approach for preventing endothelial activation in cardiovascular disorders.

Introduction

In response to various inflammatory stimuli, endothelial cells (ECs) become activated, which leads to impaired endothelium-dependent vasodilation, inadequate perfusion, vascular leakage, and inflammation. Abnormalities occur in endothelial interactions with leukocytes, platelets, and regulatory substances (Anderson, 1999; Pober et al., 2009). EC activation plays a key role in inflammation, thrombosis, and atherogenesis. Activated ECs express and activate specific adhesion molecules, such as vascular cell adhesion molecule 1 (VCAM-1) and intercellular adhesion molecule 1 (ICAM-1), which then recruit leukocytes, such as monocytes, lymphocytes, or neutrophils (Butcher, 1991). VCAM-1 and ICAM-1 have an important role in endothelial dysfunction and vascular lesion development. The recruitment of leukocytes from circulating blood is crucial in the inflammatory reaction and is a multistep process: sequential capture, rolling along and firm adhesion to the microvascular endothelium, and transmigration through the vessel wall and further migration in extravascular tissue. All of these steps are orchestrated by cell-adhesion molecules on both leukocytes and endothelial cells, and different subsets of adhesion molecules are responsible for the different steps in extravasation. The expression of adhesion molecules in the large-vessel endothelium is considered to be a key factor in

This work was supported in part by the Major National Basic Research Grant of China [Grant 2010CB912504]; the National Natural Science Foundation of China [Grants 30971063 and 81130002]; the Team Project of the Natural Science Foundation of the Guangdong Province [Grant 9351503102000001]; and the Project of the Natural Science Foundation of Guangdong Province of China [Grant 10151503102000048].

We have applied for a China patent for the synthesis and application of the compounds of SA1–SA10 used in this study: Jinhong Z, Xiaoyun Z, and Ying P (2010) inventors, Medical College of Shantou University, assignee. 1-mustard acyl-4-benzylpiperazine derivative, preparation method thereof and application of anti-free radical or anti-inflammatory activity. China patent 201010112900. 2010 Feb 9. There are no other conflicts of interest.

dx.doi.org/10.1124/mol.112.084368.

[S] This article has supplemental material available at molpharm.aspetjournals.org.

ABBREVIATIONS: BCECF, 2′,7′-bis-(2-carboxyethyl)-5-(and-6)-carboxyfluorescein; COX-2, cyclooxygenase-2; DCFH-DA, 2′,7′-dichlorfluorescein-diacetate; DHE, dihydroethidium; DPPH$^{\cdot}$, 2,2-diphenyl-1-picrylhydrazyl; DPI, dibenziodolium chloride; EC, endothelial cell; ERK, extracellular signal-regulated kinase; HUVEC, human umbilical vein endothelial cell; IκB, inhibitor κB; ICAM-1, intercellular adhesion molecule 1; JNK1, c-Jun NH_2-terminal kinase; LPS, lipopolysaccharide; MAPK, mitogen-activated protein; NF-κB/Luc, nuclear factor-κB/luciferase; PMA, phorbol 12-myristate 13-acetate; NAC, *N*-acetyl-L-cysteine; qRT-PCR, quantitative real-time reverse-transcription polymerase chain reaction; ROS, reactive oxygen species; SA, sinapic acid; SA9, 1-acetyl-sinapic acyl-4-(3′-chlorine-)benzylpiperazine; SAPK, stress-activated protein kinase; THP, human acute monocytic leukemia; TNF-α, tumor necrosis factor-α; VCAM-1, vascular cell adhesion molecule 1.

the development of atherosclerotic lesions. Upregulation of adhesion molecules with many other genes is considered to indicate EC activation.

Many endothelial functions are sensitive to the presence of reactive oxygen species (ROS) and subsequent oxidative stress (Davignon and Ganz, 2004). Pathologic processes fundamental to the development and progression of endothelial dysfunction, such as the oxidation of low-density lipoprotein, loss of bioavailable nitric oxide, and the vascular inflammatory response, are all modulated by oxidant stress (Fenster et al., 2003). Inflammatory cytokines induce EC activation by increasing ROS generation and enhancing the activity and expression of oxidative stress markers, such as NF-κB, ICAM-1, and VCAM-1 (Wagener et al., 1997; Alom-Ruiz et al., 2008; Borel et al., 2009). Tumor necrosis factor-α (TNF-α) and lipopolysaccharide (LPS) increase the expression of ICAM-1 and VCAM-1 through an NF-κB-dependent redox-sensitive mechanism in ECs (Alom-Ruiz et al., 2008; Kim et al., 2011). Thus, modulation of these processes—elimination of ROS, inhibiting the activation of NF-κB, and monocyte adherence—assumes great significance in preventing and treating EC dysfunction. Antioxidants may be an attractive therapeutic strategy to reduce endothelial dysfunction and prevent and treat cardiovascular disease (Bonetti et al., 2003; Versari et al., 2009).

Exogenous antioxidants may protect endothelial function by modulating EC-dependent vasodilation responses, homeostatic EC–monocyte interactions, the balance between pro- and antithrombotic properties, and vascular apoptotic responses (Pratico, 2005). A number of preclinical lines of evidence support this concept, and despite many studies suggesting a beneficial impact of antioxidant drugs on endothelial function, studies of the effects of classic antioxidants, such as vitamin C, vitamin E, or folic acid combined with vitamin E, have been disappointing (Munzel et al., 2010). In contrast, substances, such as statins, angiotensin-converting enzyme inhibitors, or AT1-receptor blockers, which have indirect antioxidant properties mediated by the stimulation of nitric oxide production and simultaneous inhibition of superoxide production, could improve vascular function in preclinical and clinical studies and reduce the incidence of cardiovascular events in patients with cardiovascular disease (Anderson, 1999; Shindel et al., 2008; Munzel et al., 2010). Oxidative stress remains an attractive target for cardiovascular prevention and therapy, and developing novel antioxidants from natural compounds is an interesting research direction.

One class of antioxidants is phenolic acids, many of which are natural compounds. Sinapic acid (SA) is a major component of traditional Chinese medicine found in *Ligusticum chuaxiong Hort, Descurainia sophia, and Cimicifuga foetida L.* SA retains its hydroxyl in the presence of antioxidants. In addition, the carboxylic acids in SA can be converted to amides and benzyl-substituted piperazine to increase its lipophilicity, so that it may more easily pass through a cellular plasma membrane. The SA piperazine, a novel pharmacophore, may increase new pharmacological activity. Therefore, transforming the structure of SA may be an effective way to develop new compounds with pharmacological activity.

In this study, we designed and synthesized a series of 1-erucic acyl-4-benzyl piprazine derivatives of SA (SA1–SA10). We tested the antioxidant ability of the most active compound (1-acetyl-sinapic acyl-4-(3′-chlorine-)benzyl piperazine [SA9]) on EC activation in vitro and in vivo and investigated the underlying mechanism of the protective effects in TNF-α-induced endothelial activation.

Materials and Methods

Reagents, Antibodies, and EC Culture. Antibodies for VCAM-1, ICAM-1, JNK1, p65, phosphorylated-ERK (p-ERK), and total ERK were from Santa Cruz Biotechnology (Santa Cruz, CA). Antibodies for anti-IκBα, anti-p-IκBα, and anti-p-SAPK/JNK were from Cell Signaling (Danvers, MA). Anti-ICAM-1 for immunostaining was from R&D Systems (Minneapolis, MN). Phorbol 12-myristate 13-acetate (PMA), LPS, TNF-α, dihydroethidium (DHE), bisbenzimide H, Hoechst dye 33258, Hoechst dye 33342, 2,2-diphenyl-1-picrylhydrazyl ($DPPH^{\cdot}$), 2′,7′-dichlorfluorescein-diacetate (DCFH-DA), *N*-acetyl-L-cysteine (NAC), and dibenziodolium chloride (DPI) were from Sigma-Aldrich (St. Louis, MO). 2′,7′-Bis-(2-carboxyethyl)-5-(and-6)-carboxyfluorescein (BCECF) was from Invitrogen (Carlsbad, CA). Cell culture reagents and other reagents were from HyClone Laboratories (Logan, UT), Invitrogen, or Sigma-Aldrich.

Human umbilical vein ECs (HUVECs) were isolated and cultured as previously described (Zhu et al., 2008). The investigation conforms to the principles in the Declaration of Helsinki for use of human tissue. All experiments were performed with HUVECs up to passage 6 and cultured to confluence before treatment.

$DPPH^{\cdot}$ Radical Scavenging Assay. Free radical scavenging activities were measured by use of the stable DPPH radical ($DPPH^{\cdot}$) as described elsewhere (Lum and Roebuck, 2001), with modification. In brief, 65 μM solution of $DPPH^{\cdot}$ in ethanol was added to samples at different concentrations (0.05–6.0 μM). The mixture was vortexed at room temperature for 20 minutes in dark, and the absorbance was measured at 517 nm. The capability to scavenge $DPPH^{\cdot}$ was calculated using the following equation: *% radical scavenging capacity* = $[(A_0 - A_1)/A_0] \times 100$, where A_0 is the absorbance of the control reaction and A_1 is the absorbance in the presence of sample, corrected for the absorbance of sample itself. The scavenging activity was expressed as the EC_{50} value (μM). Linear regression equations of absorbance against concentrations were determined by measuring the absorbance of 14 different concentrations of DPPH (6.5×10^{-4} M) stock solution: A (517 nm) = 7.9989C + 0.0265 (R^2 = 0. 999).

Hydroxyl Radical Scavenging Assay. Hydroxyl radical scavenging capacity was determined as described elsewhere (Ming et al., 1996). The reaction mixture contained orthophenanthroline (75 μM), acetic acid (50 μM, pH 3.0), iron(II) sulfate (75 μM), 0.1% H_2O_2, and concentrations (0.04–1.20 mM) of the test samples or the reference compound, with the exception of SA6 and SA10 (0.02–0.78 mM). After incubation for 1 hour at 37°C, the absorbance was measured at 536 nm against an appropriate blank solution. The capacity to scavenge hydroxyl radicals was calculated as follows: *% radical scavenging capacity* = $[(A_0 - A_1)/A_2] \times 100$, where A_0 is the absorbance in the presence of the sample, A_1 is the absorbance of the control without a sample, and A_2 is the absorbance of the control without a sample and H_2O_2.

Toxicity Assay for SAs in HUVECs. The effect of SA1–SA10 on cell number was analyzed using 3-(4,5-dimethylthiazol-2-yl)-2,5-diphenyltetrazolium assay for cell toxicity as described elsewhere (Zhang et al., 2006). The corrected absorbance of each sample was calculated by comparison with the untreated control.

Quantitative Real-Time Reverse-Transcription Polymerase Chain Reaction. Quantitative real-time reverse-transcription polymerase chain reaction (qRT-PCR) was performed as previously described (Zhang et al., 2010). Total cellular or tissue RNA was isolated using the TRIzol reagent method (Invitrogen) and reverse transcribed using the First Strand cDNA Synthesis kit (Thermo Fisher Scientific, Rockford, IL). The amplification reactions were in a volume of 20 μl consisting of synthesized cDNA, primers, and EasyTaq PCR Mix (Transgen Biotech, Beijing, China). Eva Green I

fluorescence (Invitrogen) was used to monitor amplification of DNA by the MX3000P qPCR detection system (Stratagene, Santa Clara, CA). Fold change in mRNA concentration was calculated using the comparative CT method. Gene expression was normalized to that of the housekeeping gene β-actin. The forward and reverse PCR primers were for GAPDH, 5′-gagtcaacggatttggtcgt-3′, 3′-ttgattttggagggatctcg-5′; ICAM-1, 5′-tggagtccagtacacggtga-3′, 5′-catagagaccccgttgccta-3′; VCAM-1, 5′-taaaatgcctgggaagatgg-3′, 5′-ctgtggtgctgcaagtcaat-3′; and cyclooxygenase 2 (COX-2), 5′-tgaaacccactccaaacaca -3′, 5′-gagaaggcttcc-cagctttt-3.

Western Blot Analysis. Protein isolation and Western blot analysis were as described elsewhere (Fu et al., 2011) with anti-ICAM-1, anti-VCAM-1, anti-JNK1, anti-p-ERK, anti-ERK, anti-IκBα, anti-p-IκBα, and anti-p-SAPK/JNK antibodies, according to standard protocols. Anti-β-actin (Bioss, Beijing, China) was used as a loading control. The protein bands were visualized by enhanced chemiluminescence (GE Healthcare, Chalfont St. Giles, Buckinghamshire, UK), and band densities were quantified using Scion Image software (Scion, Frederick, MD).

Immunofluorescence Analysis. Subconfluent HUVECs grown on coverslips were treated as indicated. The cells were fixed with 4% paraformaldehyde and immunostained with anti-p65 primary antibody and then with anti-rabbit fluorescein isothiocyanate-conjugated secondary antibody. Nuclei were stained with Hoechst dye 33342. Staining was observed under a confocal microscope.

Detection of Superoxide Anion and ROS In Situ. Generation of superoxide anion in HUVECs was measured by DHE staining and fluorescence microscopy as described elsewhere (Lefevre et al., 2007). In brief, serum-free medium containing DHE (5 μM) was applied onto each plate of cells for 20 minutes and washed. Cells then were treated with 10 ng·ml^{-1} TNF-α with or without 1 mM NAC, 20 μM DPI, and 1 μM SA9, respectively, for 20 minutes and examined under an inverted fluorescence microscopy. DHE fluorescence intensity was measured by use of a fluorescence microplate reader (BioTek; Gen5) at 485/620 nm. Generation of ROS in HUVECs was measured by DCFH-DA staining with use of a fluorescence microplate reader (BioTek; Gen5) with wavelength 485/528 nm and fluorescence microscopy (Corda et al., 2001). Generations of superoxide anion and ROS in mice ears were measured by DHE and DCFH-DA staining as described elsewhere. Generation of superoxide anion and ROS in mouse ears was measured using DHE and DCFH-DA staining separately. In brief, frozen sections were then incubated with 5 μM DHE or 10 μM DCFH-DA in phosphate-buffered saline at room temperature in the dark for 30 minutes and then coverslipped with fluorescent mounting medium. Staining was observed with use of the AxioVision Imaging System (Carl Zeiss MicroImaging GmbH, Jena, Germany).

Cell Adhesion Assay. Cell adhesion assay was performed as described elsewhere (Fu et al., 2010) with modifcation.In brief, HUVECs were pretreated with 1 μM SA9 for 30 minutes, then 10 ng·ml^{-1} TNF-α for 8 hours. THP (human acute monocytic leukemia)-1 cells were stimulated with or without 5 nM PMA for 24 hours and then labeled with fluorescence dye (BCECF). The treated HUVECs and THP-1 cells were coincubated for 15 minutes. Nonadhering cells were washed off, and adhered THP-1 cells were counted under a fluorescence microscope.

Luciferase Activity Assay. For transient transfection, 5×NF-κB/luciferase (Luc) plasmid was transfected into Hy926 cells with use of the jetPEI method (PolyPlus, Illkirch, France) 24 hours before further treatment (Dang et al., 2009). Cells were then subjected to various treatments as indicated and then were lysed to measure luciferase and β-galactosidase reporter activities. Luciferase activity was normalized to internal control β-galactosidase activity.

Animal Care and Experimental Procedure. The investigation conformed to the *Guide for the Care and Use of Laboratory Animals* published by the US National Institutes of Health (NIH Publication No. 85-23, revised 1996). C57B mice were from the Peking University Health Science Center. BALB/c mice were from the Guangzhou First Military Medical University Animal Center [license no.: SCXK (Guangdong) 2006-0015, 2006B008]. All experimental protocols were approved by the University Institutional Animal Care and Use Committee.

The model of croton oil–induced ear edema and inflammation was as described elsewhere (Conforti et al., 1991). BALB/c mice (male, 25–30 g) were randomly divided into four groups (n = 8 each). The nonsteroidal anti-inflammatory drug ibuprofen was used as a reference. The test sample was orally administered (0.2 ml·10 g^{-1} body weight) 60 minutes before croton oil–induced ear edema. Croton oil was applied (1%, 50 μl per mouse) topically on the right ear pinna of mice, and the left pinna was used as control. The mice were killed 4 hours later; both ears were removed, and circular sections (8 mm diameter) of ears were punched out with the use of a cork borer and weighed. Edema was quantified as the difference in weight between the 2 ear pinnas. Anti-inflammatory activity was evaluated as percentage inhibition in the treated animals relative to controls as follows: inhibition (%) = [(Rc-Lt)/Rc]×100%, where Rc is mean edema of control mice and Lt is mean edema of treated mice (Olajide et al., 2000). Ear thickness was analyzed using NIH ImageJ. Frozen sections of mice ears were prepared for DHE, DCFH, and hematoxylin and eosin staining.

For face-to-face immunostaining of aortas, C57B mice were fed 50 mg·kg^{-1} SA9 for 1 hour, and then inflammation was induced by intraperitoneal injection of LPS (10 mg·kg^{-1} body weight) for 8 hours before mice were killed (Garrean et al., 2006). Immunostaining for ICAM-1 in aortic intima of mice was as described elsewhere (Verna et al., 2006). After perfusion fixation and dissection, aortas were incubated with 20% goat serum, then mouse anti-ICAM-1 antibody at 4°C overnight. Secondary antibody was Cy3-labeled goat anti-mouse antibody.

Statistical Analysis. Quantitative data are expressed as mean ± S.D. Data were analyzed using regression analysis, one-way analysis of variance, and unpaired Student's t test. $P < 0.05$ was considered to be statistically significant. For nonquantitative data, results are representative of at least three independent experiments.

Results

Synthesis and Identification of SA1–SA10. To determine the most active compound of SA, we designed and synthesized a series of 1-erucic acyl-4-benzyl piprazine derivatives (SA1–SA10) from synthesized 4-substituted -benzyl piperazine (Supplemental Fig. 1A) and its derivatives (Supplemental Fig. 1B), named as compounds c1–c10 (Supplemental Table 1). Figure 1A shows the synthesis and determination of the chemical structure and substituents of SA1–SA10. The detailed procedure and the physical constants of the compounds SA1–SA10 are listed in Supplemental Methods and Supplemental Table 2. All structures of SA1–SA10 were identified by elemental analysis, mass spectrometry, ^{1}H NMR, and infrared absorption spectra (Supplemental Tables 3–5). The purity of SA1–SA10 was ≥98.47, as determined by high-performance liquid chromatography (Supplemental Table 6).

SA–SA10 Had High DPPH Content and Hydroxyl Free Radical Scavenging Activity. The stable DPPH model is widely used to evaluate antioxidant activity in a relatively short time (Villano et al., 2007). DPPH assay was used to preliminarily screen for antioxidant activity of SA–SA10. The DPPH radical scavenging activities of SA–SA10 were concentration dependent (Supplemental Fig. 2A), as seen by the high correlation coefficients ($R^2 > 0.90$; $P < 0.05$; linear range, 0–150 μM) by logarithmic regression analysis (Supplemental Table 7). SA–SA10 at 150 μM all showed DPPH$^{\cdot}$ scavenging rates >90%. The EC_{50} value, widely used to measure free radical scavenging activity, when low indicates high antioxidant activity (Maisuthisakula et al.,

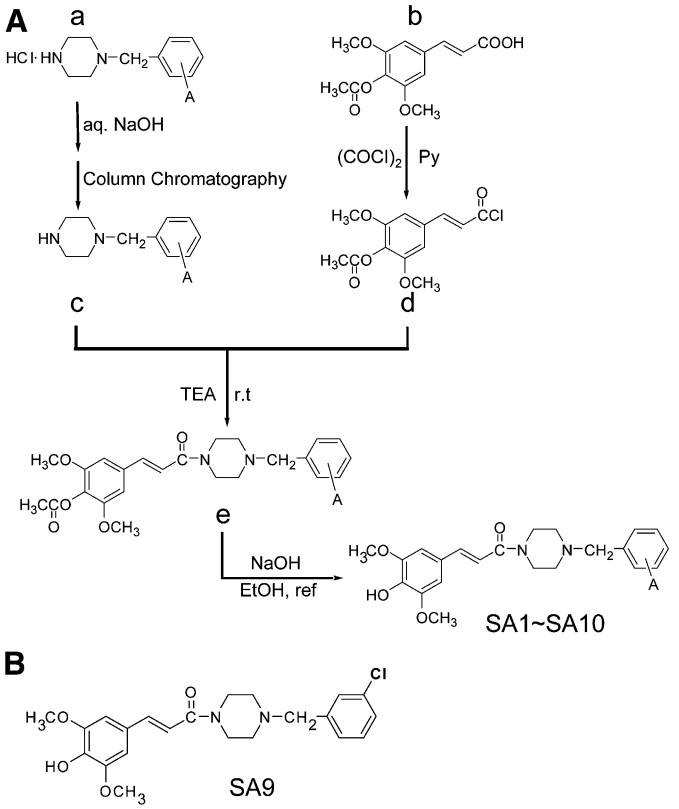

Fig. 1. Synthesis, chemical structures, and substituents of sinapic acid derivatives (SA1–SA10). (A) Synthesis of SA (a), acetyl sinapic acid (b), acetyl sinapic chloride (c), piperazine dihydrochloride monohydrate (d), and *N*-benzyl piperazine hydrochloride (e) and synthesis of SA1–SA10. (B) Structure of SA9, 1-acetyl-sinapic acyl-4-(3′-chlorine-) benzylpiperazine.

2007). The EC_{50} values (Supplemental Table 7) were organized by four groups ($P<0.05$), as follows: SA<SA10 < SA1, SA2, SA8, and SA9 < SA4, SA6, SA7, SA3, SA5. Thus, SA–SA10 showed high proton-donating ability on $DPPH^{\cdot}$ to form stable DPPH molecules.

Hydroxyl radicals are the major active oxygen species causing lipid peroxidation and enormous biologic damage. The hydroxyl radical scavenging activities of SA–SA10 were also concentration dependent (Supplemental Fig. 2B), as seen by the high correlation coefficients ($R^2 > 0.90$; $P < 0.05$; linear range, 79.43–602.56 μM) (Supplemental Table 8). The EC_{50} values allowed for dividing the derivatives by 7 groups, as follows: SA6 < SA10 < SA4, SA5, SA7 < SA1, SA8, and SA9 < SA3 < SA<SA2. Thus, SA–SA10 showed strong activity to inhibit the generation of hydroxyl radicals from the fenton reaction.

Effect of SA–SA10 on the Inhibition of Croton Oil–induced Ear Edema in Mice. To screen the anti-inflammatory properties of the compounds SA–SA10 in vivo, we created a mouse model of croton oil–induced edema in ears. With the exception of SA and SA7, most SAs at 100 or 200 $mg \cdot kg^{-1}$ had effective anti-inflammatory activity (Table 1). Compared with the nonsteroidal anti-inflammatory drug ibuprofen, compounds SA9, SA6, SA8, SA1, and SA4 showed higher anti-inflammatory ability, with SA9 having the strongest inhibitory activity at 200 $mg \cdot kg^{-1}$ (45.65% inhibition). Figure 1B shows the chemical structure of SA9.

Effect of SA1–SA10 on TNF-α-Induced Pre-Inflammatory Reaction in ECs. To explore the mechanism of the anti-inflammatory ability of SA1–SA10, cultured HUVECs were treated with 10 $ng \cdot ml^{-1}$ TNF-α and a 1 μM concentration of each SA derivative. The TNF-α-induced upregulation of ICAM-1 was significantly attenuated by SA3–SA8, SA9, and SA10 (Fig. 2A). Of note, only SA6 and, especially, SA9 significantly decreased the expression of VCAM-1 with TNF-α treatment (Fig. 2B). In contrast, no SA derivatives had an effect on the regulation of COX-2 (Fig. 2C). At concentrations <50 μM, SA1–SA10 had little effect on cell survival and did not cause cytotoxicity in HUVECs, as analyzed by 3-(4,5-dimethylthiazol-2-yl)-2,5-diphenyltetrazolium assay (Supplemental Fig. 2C). The effect of SA9 on inhibiting the expression of ICAM-1 and VCAM-1 was further confirmed at the protein level (Fig. 3A). Thus, the SA derivatives, especially SA9, possessed anti-inflammatory abilities, at least in part, by inhibiting the expression of ICAM-1 and VCAM-1 in ECs. An antioxidant NAC was reported to efficiently reduce the expression of adhesion molecules in ECs (Faruqi et al., 1997). In this study, we used NAC as a positive control (Fig. 3A); the similar inhibitory effect of SA9 and NAC on TNF-α-induced VCAM-1 and ICAM-1 expression was observed.

TABLE 1

Effect of compounds at 100 or 200 $mg \cdot kg^{-1}$ on croton oil–induced ear edema in mice

Analysis of variance and Newman-Keuls multiple comparison test were used. Data are mean ± S.D. (n = 8) or percentage.

Compound	Edema (100 $mg \cdot kg^{-1}$)	Edema (200 $mg \cdot kg^{-1}$)	Inhibition (100 $mg \cdot kg^{-1}$)	Inhibition (200 $mg \cdot kg^{-1}$)
	mg	%		
Ctrl	14.08 ± 1.11	14.08 ± 1.11	—	—
Croton oil	19.23 ± 1.36*	19.23 ± 1.36*	—	—
Ibu	13.32 ± 2.83$^{\#}$	11.37 ± 4.16$^{\#\#}$	21.33	32.86
SA	23.6 ± 3.54^{ns}	20.00 ± 1.72^{ns}	−39.41	−18.14
SA1	14.87 ± 2.38^{ns}	10.88 ± 4.48$^{\#\#}$	12.18	35.71
SA2	14.72 ± 2.30^{ns}	14.42 ± 3.93$^{\#}$	13.07	14.84
SA3	14.88 ± 2.78^{ns}	14.30 ± 2.58$^{\#}$	12.08	15.53
SA4	14.17 ± 3.22^{ns}	11.02 ± 2.68$^{\#\#}$	16.32	34.92
SA5	13.13 ± 3.75$^{\#}$	11.92 ± 2.35$^{\#\#}$	22.42	29.61
SA6	13.22 ± 2.76$^{\#}$	9.88 ± 3.90$^{\#\#}$	21.93	41.62
SA7	21.93 ± 3.29^{ns}	18.60 ± 2.63^{ns}	−29.56	−9.87
SA8	13.65 ± 2.17$^{\#}$	9.90 ± 3.79$^{\#\#}$	19.37	41.52
SA9	12.97 ± 3.38$^{\#}$	9.20 ± 4.27$^{\#\#}$	23.4	45.65
SA10	14.78 ± 3.87^{ns}	13.63 ± 4.52$^{\#}$	12.67	19.47

ns, not significant.

*$P < 0.05$ versus control; ##$P < 0.01$; #$P < 0.05$ versus croton oil.

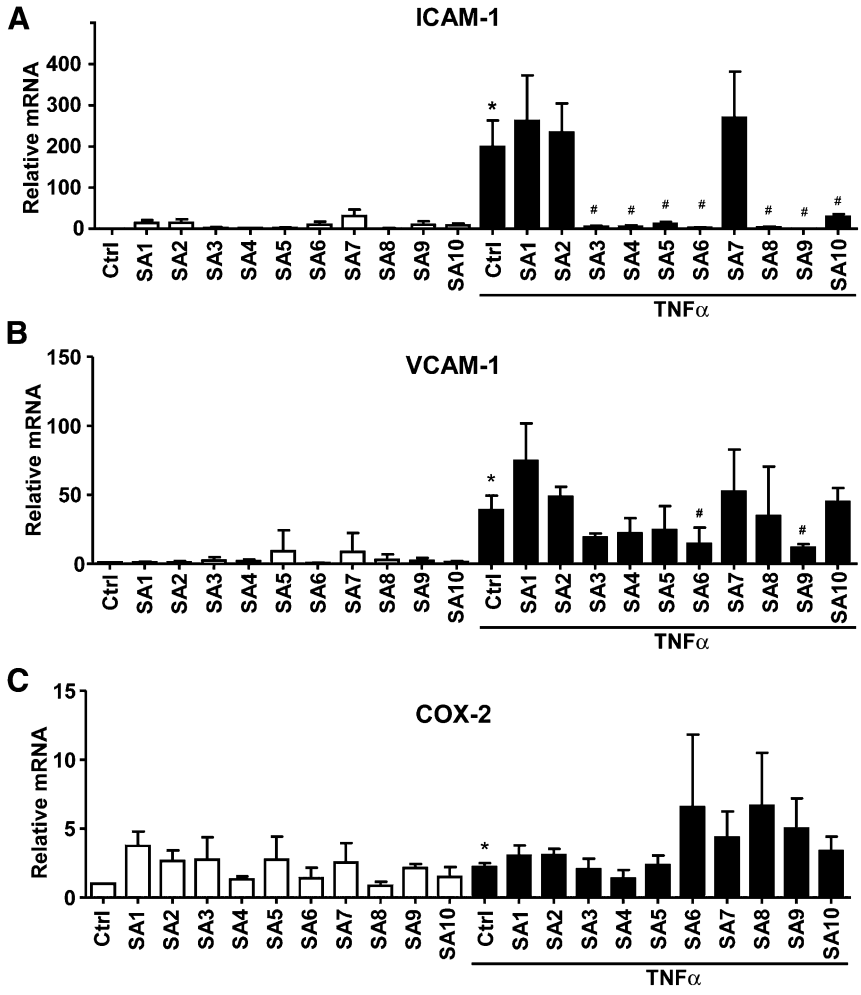

Fig. 2. Effect of SA1–SA10 on TNF-α inhibition of intracellular ICAM-1, VCAM-1, and COX-2 in HUVECs. HUVECs were pretreated with 10 ng·ml^{-1} TNF-α and 1 μM SA1–SA10 for 6-hour reverse-transcription polymerase chain reaction analysis of mRNA levels of human ICAM-1 (A), VCAM-1 (B), and COX-2 (C). GAPDH cDNA was an internal control. Data are mean ± S.D. of mRNA relative to that of GAPDH from three independent experiments. *P < 0.05 versus control (Ctrl); #P < 0.05; ##P < 0.01 versus TNF-α.

SA9 Attenuated TNF-α–Induced Adhesion of THP-1 Cells to ECs. Because the expression of adhesion molecules on ECs is a prerequisite for adhesion of leukocytes, we investigated the effect of SA9 on TNF-α–induced THP-1 cell adhesion to HUVECs. Untreated or PMA-activated THP-1 cells were used in the monocyte binding assay to indicate the function of VCAM-1 and ICAM-1. Pretreating HUVECs with 1 μM SA9 significantly reduced both ICAM-1- and VCAM-1-mediated monocyte adhesion induced by TNF-α (Fig. 3, B and C).

SA9 Inhibited Inflammation-Induced Oxidative Stress in ECs. To further explore the mechanism by which SA9 exerted its anti-inflammatory effect, we measured TNF-α-induced oxidative stress by superoxide anion generation and ROS level in HUVECs by DHE and DCFH-DA staining, respectively. The antioxidants NAC and DPI served as the positive control. Exposure to 10 ng·ml^{-1} TNF-α increased superoxide anion generation and ROS levels in HUVECs (Fig. 4, A and B). However, pretreatment with NAC, DPI, and SA9 showed similar effect to prevent the increased oxidative stress in ECs. To study the antioxidant effects of SA9 in vivo, we measured mouse ear edema in a croton oil–induced mouse model. Croton oil induced blood vessel dilation, congestion, thickness of mouse ear pieces, and infusion of inflammatory cells (Fig. 4C); all were significantly inhibited by SA9. The superoxide anion level and generation of ROS induced by proinflammatory edema were significantly reduced by SA9 (Fig. 4, D and E).

The Anti-Inflammatory Effects of SA9 Were through Inhibiting of NF-κB Activation. As demonstrated above, SA9 exerted its anti-inflammatory effect by inhibiting TNF-α-induced oxidative stress and the expression of cell adhesion molecules but not COX-2. Because upregulation of cell adhesion molecules and activation of NF-κB can be induced by TNF-α (Paik et al., 2002), we next studied the involvement of NF-κB in the anti-inflammatory effects of SA9 in ECs. The transfection results in Fig. 5A revealed that treatment of TNF-α could activate NF-κB/Luc in ECs, which was largely attenuated by SA9 pretreatment. In addition, immunofluorescence analysis revealed that the nuclear translocation of p65, a subunit of NF-κB and marker of its activation, was significantly inhibited by SA9 (Fig. 5B). Furthermore, Western blot results showed that, with SA9 pretreatment, the phosphorylation of IκB was significantly inhibited. AP-1 is another redox-sensitive transcriptional factor and the phosphorylation of JNK and ERK upstream of AP-1 activation. Therefore, we also detected the phosphorylation of JNK and ERK and found that phosphorylation of both JNK and ERK was increased by TNF-α, which could be reduced by SA9 to a certain degree (Fig. 5C). Thus, the anti-inflammatory effects of SA9 were by inhibition of NF-κB, but the involvement of AP-1 could not be excluded.

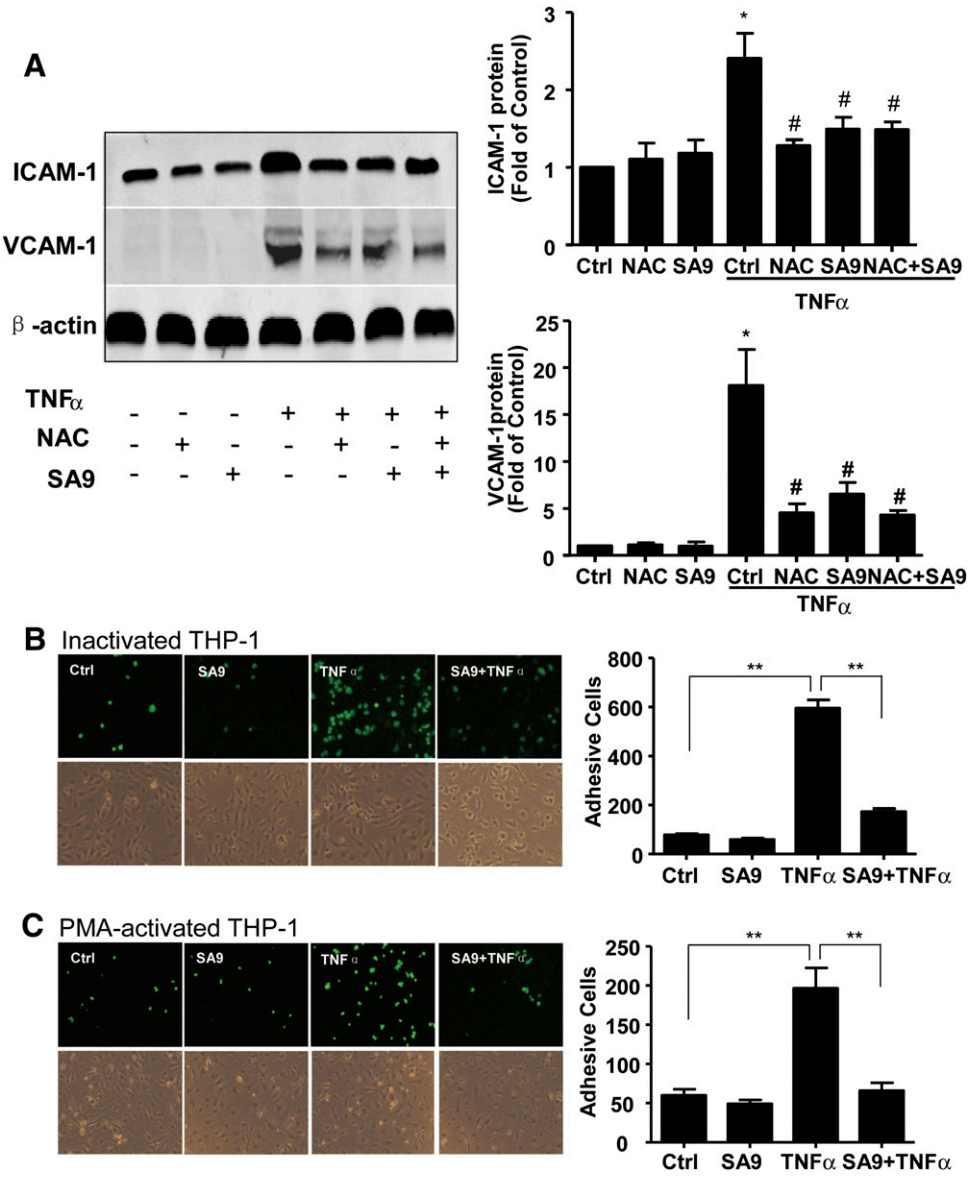

Fig. 3. The inhibitory effect of SA9 on TNFα–induced adhesion molecules and monocyte adhesion to ECs. (A) HUVECs were pretreated with 1 μM SA9 or 1 mM NAC for 30 minutes, and then with 10 ng·ml^{-1} TNF-α for 8 hours. Whole cells were lysed, and ICAM-1 and VCAM-1 protein were measured by Western blot analysis. β-Actin was a loading control. Data are mean ± S.D. of the protein normalized to that of β-actin from three independent experiments. *$P < 0.05$ versus control (Ctrl); #$P < 0.05$ versus TNF-α. (B) HUVECs were pretreated with 1 μM SA9 for 30 minutes and then treated with 10 ng·ml^{-1} TNF-α for 8 hours (C). THP-1 cells were stimulated with or without PMA and then labeled with fluorescence dye. Cell adhesion assay was performed. Representative results and quantitative results show fold change in cell adhesion, compared with untreated controls. Data are the mean ± S.D. of four independent experiments, each performed in triplicate. *$P < 0.05$; **$P < 0.01$.

SA9 Inhibited the LPS-Induced Expression of ICAM-1 in Mouse Aortic Intima. To investigate whether SA9 possesses anti-inflammatory effects in vivo, we examined LPS-induced expression of ICAM-1 in the aortic endothelium of C57 mice. Face-to-face immunofluorescence staining showed that the expression of ICAM-1 significantly increased in the aortic endothelium when animals were injected LPS to induce a systemic inflammation; the LPS-mediated upregulation of ICAM-1 was significantly attenuated with SA9 administration (Fig. 6). Thus, SA9 had an anti-inflammatory effect by inhibiting the expression of adhesion molecules in vascular endothelium in vitro and in vivo.

Discussion

SA is a phenylpropanoid compound found in natural herbs and high-bran cereals. It was reported to have moderate antioxidant and anti-inflammatory efficacy (Yun et al., 2008; Galano et al., 2011; Kwak et al., 2013). To improve the antioxidant and anti-inflammatory properties and capitalize on other pharmacological functions of SA, we designed and synthesized 10 SA derivatives by varying the substitution of methyl, methoxy, and chloro groups at ortho, meta, and para positions of the phenyl ring. All 10 derivatives showed certain antioxidant activities in a cell-free system, but when tested on cultured cells, SA9 showed higher free radical scavenge activities and stronger inhibitory effects on TNF-α-induced upregulation of adhesion molecules in ECs. Furthermore, SA9 inhibited the monocyte/macrophage adhesion to ECs and the LPS-induced expression of ICAM-1 in mouse aortic intima. The mechanism was by inhibiting oxidative stress and NF-κB activation in ECs.

Preliminary screening of the antioxidant and anti-inflammatory ability of the 10 SA derivatives involved in investigating scavenging hydroxyl radicals and DPPH· in cell-free system, expression of adhesion molecules in cultured ECs, and croton oil–induced ear edema in mouse model. Although almost all compounds could scavenge hydroxyl radicals and DPPH· and possessed topical anti-inflammatory properties and excellent biocompatibility, SA9 had stronger

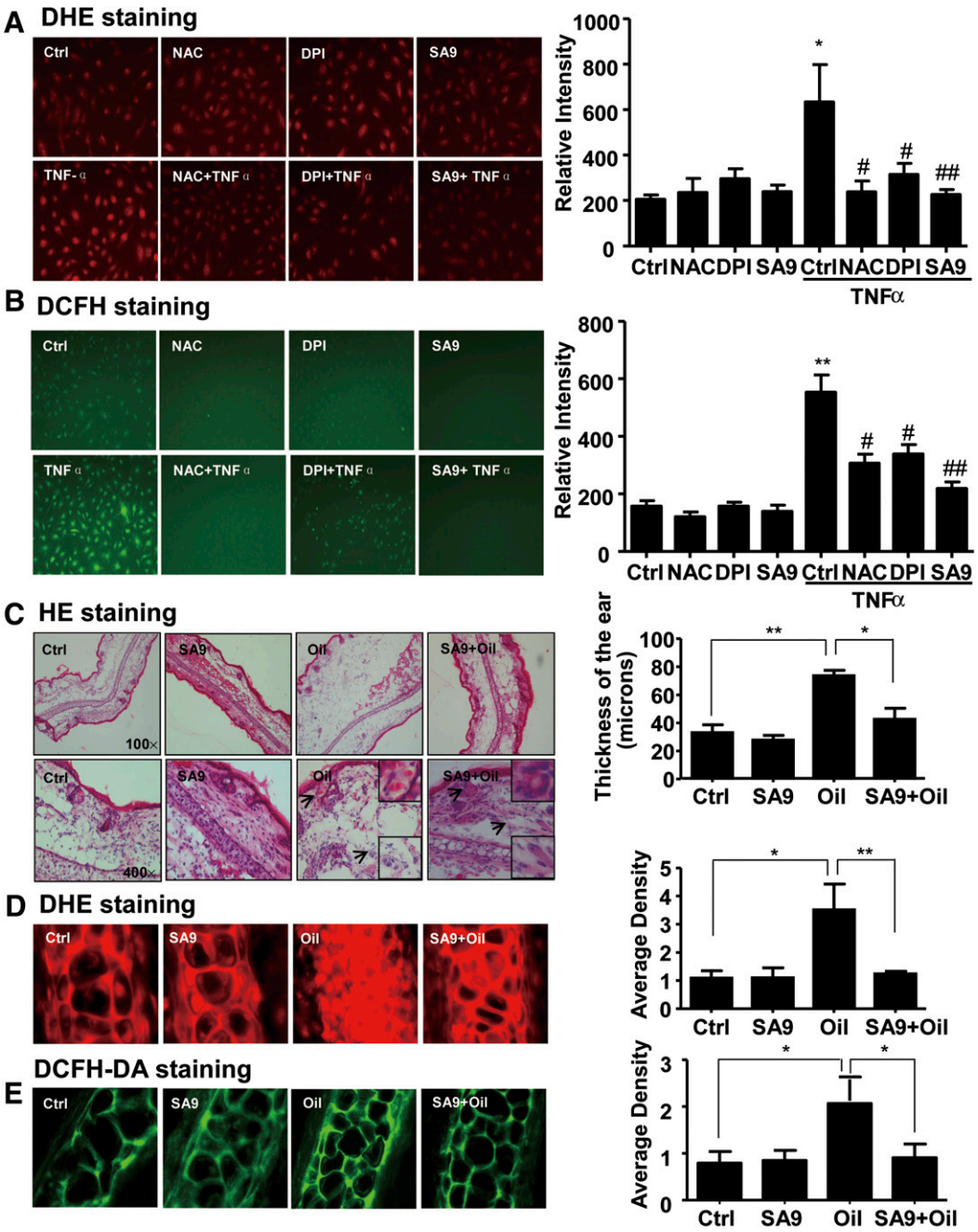

Fig. 4. SA9 inhibited inflammation-induced oxidative stress in vitro and in vivo. (A and B) HUVECs were pretreated with 1 mM NAC, 20 μM DPI, or 1 μM SA9 for 30 minutes, then with 10 ng·ml^{-1} TNF-α for 30 minutes in the DCFH-DA assay and for 20 minutes in the DHE assay. Quantification of DCFH-DA and DHE images was from four different experiments with use of a fluorescence microplate reader (BioTek, Gen5). *$P < 0.05$; **$P < 0.01$ versus control (Ctrl); #$P < 0.05$; ##$P < 0.01$ versus TNF-α. (C–E) Croton oil (1%, 50 μl per mouse) was applied on the right ear pinna of BALB/c mice, and the left pinna was used as control. The mice were euthanized 4 hours after croton oil was applied, and then ears were removed. (C) Cross-sections of the ears with HE staining (magnification: 100× and 400×) and quantification. Arrows indicated blood vessels dilated and congested and infiltrated inflammatory cells in the dermis. Superoxide anion level measured by DHE staining (D) and ROS levels measured by DCFH-DA staining (E). Magnification: 400×. Data are mean ± S.D. from 6 mice (right). *$P < 0.05$; **$P < 0.01$.

antioxidant and anti-inflammatory activity in ECs and animal models.

The fat-soluble and site of substitution on benzyl are important factors affecting antioxidant and anti-inflammatory activity. Chlorine atoms and the meta-substituted position increased the activity of the compounds. Theoretically, a compound with high fat solubility has better activity. Indeed, the structure of SA9 is the meta-substitution of the benzene ring by the chlorine atom. Thus, SA9 should have efficient antioxidation activity, which we confirmed.

Oxidative stress has long been recognized as an important contributor to cardiovascular disease. The production of ROS (free radicals and peroxides) is a particularly detrimental aspect of oxidative stress. Numerous clinical studies showed that increased vascular oxidative stress is strongly associated with cardiovascular events in patients with coronary artery

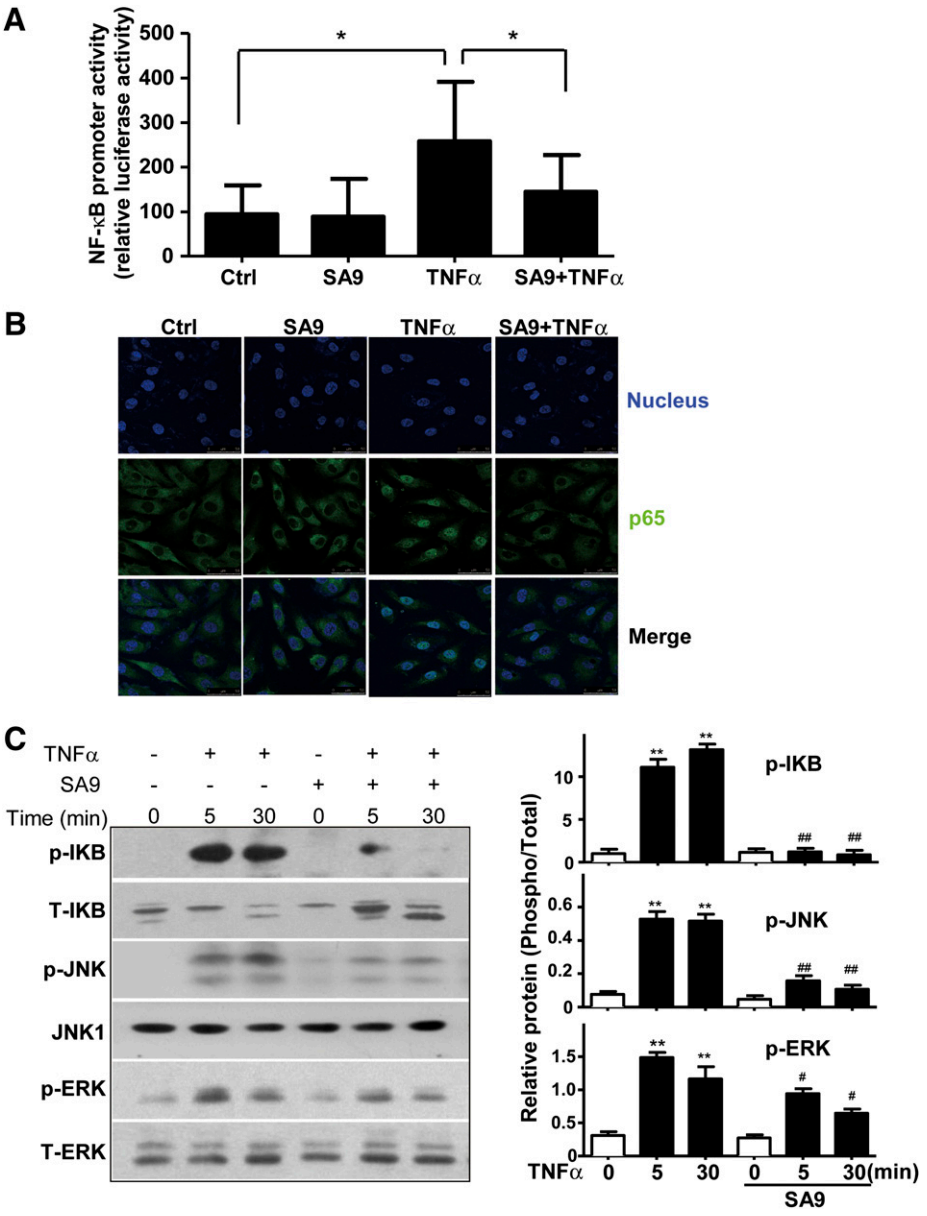

Fig. 5. The anti-inflammatory effects of SA9 was by inhibiting of NF-κB. (A) Hy926 cells were transfected with NF-κB/Luc for 24 hours and then treated with 10 ng·ml^{-1} TNF-α and 1 μM SA9 for another 24 hours. β-Galactosidase plasmid was cotransfected as a transfection control. Luciferase activities were normalized to that of β-galactosidase. Data are mean ± S.D. of the relative luciferase activities from three independent experiments, each performed in triplicate (*P < 0.05). (B) HUVECs were treated with 10 ng·ml^{-1} TNF-α and 1 μM SA9 for 2 hours. NF-κB subunit p65 was stained with rabbit anti-p65 and anti-rabbit fluorescein isothiocyanate-conjugated secondary antibody (green), and Hoechst dye was used for nuclear staining (blue). The images were observed using confocal fluorescence microscopy. Results are representative of three separate experiments. (C) HUVECs were pretreated with 10 ng·ml^{-1} TNF-α and 1 μM SA9 for 5 and 30 minutes. Western blot analysis of protein levels of p-IκB, t-IκB, p-JNK, JNK1, p-ERK, and t-ERK. Results are representative of three independent experiments. Bar graphs show the band density ratio of phosphorylated to total protein levels (p-IκB/t-IκB, p-JNK/JNK1, and p-ERK/t-ERK), respectively. **P < 0.01 versus control (Ctrl). ##P < 0.01 versus TNF-α.

disease (Heitzer et al., 2001). Here, we found that SA9 has ROS scavenger property and could efficiently reduce superoxide anions in ECs. Additional results indicated that SA9 has strong antioxidant activity and protects ECs against activation and injury by ROS. Inflammatory status is a risk factor of cardiovascular disease. The expression of cell adhesion molecules, such as VCAM-1 and ICAM-1, mediates monocyte/macrophage adhesion and the consequent processes in initiating atherogenesis (Trerotola et al., 2010). We found that SA9 could significantly inhibit the TNF-α-induced ROS generation, upregulation of ICAM-1 and VCAM-1 in ECs, and blocked monocyte adhesion to ECs, similar as the effect of NAC and DPI, well-known antioxidants. It was reported that NAC suppressed TNF-α-stimulated expression of adhesion molecules by inhibiting ROS and NF-κB activity. (Sakurada et al., 1996; Zafarullah et al., 2003). In addition, our preclinical animal model confirmed the anti-inflammatory properties of SA9 in inhibiting the expression of ICAM-1 in the aortic endothelium. Our results are supported by numerous studies showing that reducing intracellular ROS production could inhibit monocyte adhesiveness to ECs (Lin et al., 2005; Paine et al., 2010).

NF-κB, a redox-sensitive transcription factor, could be activated by oxidative stress and is involved in proinflammatory cytokine production (Pueyo et al., 2000). Therefore, we proposed that the anti-inflammatory effects of SA9 were based on the inhibition of NF-κB activation. SA9 potently suppressed TNF-α-mediated activation of NF-κB and the nuclear translocation of p65, a subunit of NF-κB, in HUVECs. Thus, the mechanism of the anti-inflammatory effects of SA9 depended on the inhibition of ROS and NF-κB. However, SA9 did not prevent the TNF-α-induced upregulation of COX-2. Regulation of COX-2 by TNF-α was previously found to be mediated by both MAPK and NF-κB (Paik et al., 2002). The regulation of COX-2 by MAPK and NF-κB is by separate signaling pathways, and p38 MAPK but not NF-κB participates in the

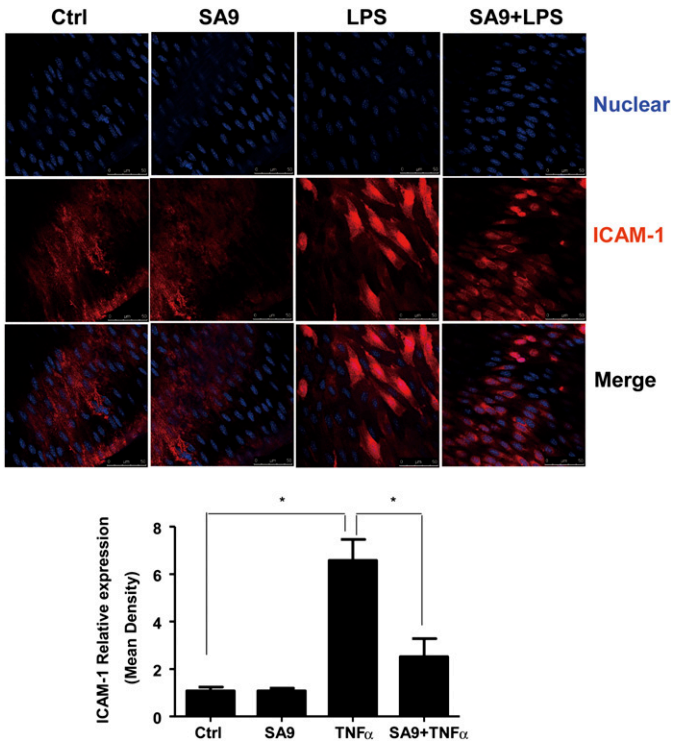

Fig. 6. SA9 inhibited the expression of ICAM-1 on mouse aortic intima induced by LPS in vivo. C57B mice were fed 50 mg·kg^{-1} body weight SA9 for 1 hour; then, the inflammation was induced by intraperitoneal injection of LPS (10 mg·kg^{-1} body weight) for 8 hours. Sections of aortic endothelial underwent en face immunostaining for ICAM-1. The red fluorescent staining indicates surface ICAM-1 immunoreactivity, and blue staining represents nuclear staining by Hoechst dye 33258. Images are representative of results from six mice. Bar graphs show the mean density of ICAM-1 relative expression. *$P < 0.05$.

regulation of COX-2 mRNA stability (Singer et al., 2003). We found that SA9 mainly inhibited TNF-α-induced phosphorylation of IKB but also attenuated phosphorylation of JNK and ERK to a certain degree, which suggests the involvement of the AP-1 pathway (c-Jun/c-Fos). Our results also indicate the induction of COX-2 and VCAM-1/ICAM-1 by cytokines via different mechanisms.

In conclusion, we demonstrated that SA9, a new SA derivative, could efficiently prevent endothelial oxidative stress in vitro and in vivo. In addition, SA9 could inhibit the TNF-α-induced NF-κB activation and the expression of cell adhesion molecules for a potential endothelial protective effect. SA9 may provide a new therapeutic approach for preventing endothelial activation in cardiovascular disorders.

Authorship Contributions

Participated in research design: Zhu, Zheng, Zeng.

Conducted experiments: Zeng, Fu, Su, Sun, Zhang, Hou.

Contributed new reagents or analytic tools: Zeng, Fu, Su, Sun, Zhang, Hou.

Performed data analysis: Zeng, Fu, Su, Sun, Zhang, Zhu.

Wrote or contributed to the writing of the manuscript: Zeng, Fu, Sun, Zhu.

References

Alom-Ruiz SP, Anilkumar N, and Shah AM (2008) Reactive oxygen species and endothelial activation. *Antioxid Redox Signal* **10**:1089–1100.

Anderson TJ (1999) Assessment and treatment of endothelial dysfunction in humans. *J Am Coll Cardiol* **34**:631–638.

Bonetti PO, Lerman LO, and Lerman A (2003) Endothelial dysfunction: a marker of atherosclerotic risk. *Arterioscler Thromb Vasc Biol* **23**:168–175.

Borel JC, Roux-Lombard P, Tamisier R, Arnaud C, Monneret D, Arnol N, Baguet JP, Levy P, and Pepin JL (2009) Endothelial dysfunction and specific inflammation in obesity hypoventilation syndrome. *PLoS ONE* **4**:e6733.

Butcher EC (1991) Leukocyte-endothelial cell recognition: three (or more) steps to specificity and diversity. *Cell* **67**:1033–1036.

Conforti A, Caliceti P, Sartore L, Schiavon O, Veronese F, and Velo GP (1991) Anti-inflammatory activity of monomethoxypolyethylene glycol superoxide dismutase on adjuvant arthritis in rats. *Pharmacol Res* **23**:51–56.

Corda S, Laplace C, Vicaut E, and Duranteau J (2001) Rapid reactive oxygen species production by mitochondria in endothelial cells exposed to tumor necrosis factor-alpha is mediated by ceramide. *Am J Respir Cell Mol Biol* **24**:762–768.

Dang H, Liu Y, Pang W, Li C, Wang N, Shyy JY, and Zhu Y (2009) Suppression of 2,3-oxidosqualene cyclase by high fat diet contributes to liver X receptor-alpha-mediated improvement of hepatic lipid profile. *J Biol Chem* **284**:6218–6226.

Davignon J and Ganz P (2004) Role of endothelial dysfunction in atherosclerosis. *Circulation* **109**(23, Suppl 1)III27–III32.

Faruqi RM, Poptic EJ, Faruqi TR, De La Motte C, and DiCorleto PE (1997) Distinct mechanisms for N-acetylcysteine inhibition of cytokine-induced E-selectin and VCAM-1 expression. *Am J Physiol* **273**:H817–H826.

Fenster BE, Tsao PS, and Rockson SG (2003) Endothelial dysfunction: clinical strategies for treating oxidant stress. *Am Heart J* **146**:218–226.

Fu C, He J, and Li C, Shyy JY, and Zhu Y (2010) Cholesterol increases adhesion of monocytes to endothelium by moving adhesion molecules out of caveolae. *Biochim Biophys Acta* 1801:702–710.

Fu Y, Hou Y, Fu C, Gu M, Li C, Kong W, Wang X, Shyy JY, and Zhu Y (2011) A novel mechanism of γ/δ T-lymphocyte and endothelial activation by shear stress: the role of ecto-ATP synthase β chain. *Circ Res* **108**:410–417.

Galano A, Francisco-Márquez M, and Alvarez-Idaboy JR (2011) Mechanism and kinetics studies on the antioxidant activity of sinapinic acid. *Phys Chem Chem Phys* **13**:11199–11205.

Garrean S, Gao XP, Brovkovych V, Shimizu J, Zhao YY, Vogel SM, and Malik AB (2006) Caveolin-1 regulates NF-kappaB activation and lung inflammatory response to sepsis induced by lipopolysaccharide. *J Immunol* **177**:4853–4860.

Heitzer T, Schlinzig T, Krohn K, Meinertz T, and Münzel T (2001) Endothelial dysfunction, oxidative stress, and risk of cardiovascular events in patients with coronary artery disease. *Circulation* **104**:2673–2678.

Kim YM, Kim MY, Kim HJ, Roh GS, Ko GH, Seo HG, Lee JH, and Chang KC (2011) Compound C independent of AMPK inhibits ICAM-1 and VCAM-1 expression in inflammatory stimulants-activated endothelial cells in vitro and in vivo. *Atherosclerosis* **219**:57–64.

Kwak SY, Yang JK, Choi HR, Park KC, Kim YB, and Lee YS (2013) Synthesis and dual biological effects of hydroxycinnamoyl phenylalanyl/prolyl hydroxamic acid derivatives as tyrosinase inhibitor and antioxidant. *Bioorg Med Chem Lett* **23**:1136–1142.

Lefèvre J, Michaud SE, Haddad P, Dussault S, Ménard C, Groleau J, Turgeon J, and Rivard A (2007) Moderate consumption of red wine (cabernet sauvignon) improves ischemia-induced neovascularization in ApoE-deficient mice: effect on endothelial progenitor cells and nitric oxide. *FASEB J* **21**:3845–3852.

Lin SJ, Shyue SK, Hung YY, Chen YH, Ku HH, Chen JW, Tam KB, and Chen YL (2005) Superoxide dismutase inhibits the expression of vascular cell adhesion molecule-1 and intracellular cell adhesion molecule-1 induced by tumor necrosis factor-alpha in human endothelial cells through the JNK/p38 pathways. *Arterioscler Thromb Vasc Biol* **25**:334–340.

Lum H and Roebuck KA (2001) Oxidant stress and endothelial cell dysfunction. *Am J Physiol Cell Physiol* **280**:C719–C741.

Maisuthisakula P, Suttajitb M, and Pongsawatmanit R (2007) Assessment of phenolic content and free radical-scavenging capacity of some Thai indigenous plants. *Food Chem Toxical* **100**:1409–1418.

Ming J, Yaxin C, Jinrong L, and Hui Z (1996) 1,10-Phenanthroline-Fe2+ oxidative assay of hydroxyl radical produced by H2O2/Fe2+. *Progress in Biochemistry and Biophysics* **23**:553–555.

Münzel T, Gori T, Bruno RM, and Taddei S (2010) Is oxidative stress a therapeutic target in cardiovascular disease? *Eur Heart J* **31**:2741–2748.

Olajide OA, Makinde JM, Okpako DT, and Awe SO (2000) Studies on the anti-inflammatory and related pharmacological properties of the aqueous extract of Bridelia ferruginea stem bark. *J Ethnopharmacol* **71**:153–160.

Paik J, Lee JY, and Hwang D (2002) Signaling pathways for TNFa-induced COX-2 expression: mediation through MAP kinases and NFkB, and inhibition by certain nonsteroidal anti-inflammatory drugs. *Adv Exp Med Biol* **507**:503–508.

Paine A, Eiz-Vesper B, Blasczyk R, and Immenschuh S (2010) Signaling to heme oxygenase-1 and its anti-inflammatory therapeutic potential. *Biochem Pharmacol* **80**:1895–1903.

Pober JS, Min W, and Bradley JR (2009) Mechanisms of endothelial dysfunction, injury, and death. *Annu Rev Pathol* **4**:71–95.

Praticò D (2005) Antioxidants and endothelium protection. *Atherosclerosis* **181**:215–224.

Pueyo ME, Gonzalez W, Nicoletti A, Savoie F, Arnal JF, and Michel JB (2000) Angiotensin II stimulates endothelial vascular cell adhesion molecule-1 via nuclear factor-kappaB activation induced by intracellular oxidative stress. *Arterioscler Thromb Vasc Biol* **20**:645–651.

Sakurada S, Kato T, and Okamoto T (1996) Induction of cytokines and ICAM-1 by proinflammatory cytokines in primary rheumatoid synovial fibroblasts and inhibition by N-acetyl-L-cysteine and aspirin. *Int Immunol* **8**:1483–1493.

Shindel AW, Kishore S, and Lue TF (2008) Drugs designed to improve endothelial function: effects on erectile dysfunction. *Curr Pharm Des* **14**:3758–3767.

Singer CA, Baker KJ, McCaffrey A, AuCoin DP, Dechert MA, and Gerthoffer WT (2003) p38 MAPK and NF-kappaB mediate COX-2 expression in human airway myocytes. *Am J Physiol Lung Cell Mol Physiol* **285**:L1087–L1098.

Trerotola M, Guerra E, and Alberti S (2010) Letter to the editor: efficacy and safety of anti-Trop antibodies, R. Cubas, M. Li, C. Chen and Q. Yao, Biochim Biophys Acta 1796 (2009) 309-1. *Biochim Biophys Acta* 1805:119–120; author reply 121–112.

Verna L, Ganda C, and Stemerman MB (2006) In vivo low-density lipoprotein exposure induces intercellular adhesion molecule-1 and vascular cell adhesion molecule-1 correlated with activator protein-1 expression. *Arterioscler Thromb Vasc Biol* **26**:1344–1349.

Versari D, Daghini E, Virdis A, Ghiadoni L, and Taddei S (2009) Endothelial dysfunction as a target for prevention of cardiovascular disease. *Diabetes Care* **32** (Suppl 2):S314–S321.

Villaño D, Fernández-Pachón MS, Moyá ML, Troncoso AM, and García-Parrilla MC (2007) Radical scavenging ability of polyphenolic compounds towards DPPH free radical. *Talanta* **71**:230–235.

Wagener FA, Feldman E, de Witte T, and Abraham NG (1997) Heme induces the expression of adhesion molecules ICAM-1, VCAM-1, and E selectin in vascular endothelial cells. *Proc Soc Exp Biol Med* **216**:456–463.

Yun KJ, Koh DJ, Kim SH, Park SJ, Ryu JH, Kim DG, Lee JY, and Lee KT (2008) Anti-inflammatory effects of sinapic acid through the suppression of inducible nitric oxide synthase, cyclooxygase-2, and proinflammatory cytokines expressions via nuclear factor-kappaB inactivation. *J Agric Food Chem* **56**:10265–10272.

Zafarullah M, Li WQ, Sylvester J, and Ahmad M (2003) Molecular mechanisms of N-acetylcysteine actions. *Cell Mol Life Sci* **60**:6–20.

Zhang D, Ai D, Tanaka H, Hammock BD, and Zhu Y (2010) DNA methylation of the promoter of soluble epoxide hydrolase silences its expression by an SP-1-dependent mechanism. *Biochim Biophys Acta* **1799**:659–667.

Zhang DH, Marconi A, Xu LM, Yang CX, Sun GW, Feng XL, Ling CQ, Qin WZ, Uzan G, and d'Alessio P (2006) Tripterine inhibits the expression of adhesion molecules in activated endothelial cells. *J Leukoc Biol* **80**:309–319.

Zhu M, Fu Y, Hou Y, Wang N, Guan Y, Tang C, Shyy JY, and Zhu Y (2008) Laminar shear stress regulates liver X receptor in vascular endothelial cells. *Arterioscler Thromb Vasc Biol* **28**:527–533.

Address correspondence to: Dr. Yi Zhu, Department of Physiology and Pathophysiology, Tianjin Medical University, 20 Qixiangtai Rd., Tianjin, 300070, China. E-mail: zhuyi@tmu.edu.cn